Hyaluronan Concentration within a 3D Collagen Matrix Modulates Matrix Viscoelasticity, But Not Fibroblast Response

S.T. Kreger[1] and **S.L. Voytik-Harbin**[1,2]

[1]Weldon School of Biomedical Engineering, College of Engineering, Purdue University, West Lafayette, Indiana, USA

[2]Department of Basic Medical Sciences, School of Veterinary Medicine, Purdue University, West Lafayette, Indiana, USA

Abstract

The use of 3D extracellular matrix (ECM) microenvironments to deliver growth-inductive signals for tissue repair and regeneration requires an understanding of the mechanisms of cell-ECM signaling. Recently, hyaluronic acid (HA) has been incorporated in collagen matrices in an attempt to recreate tissue specific microenvironments. However, it is not clear how HA alters biophysical properties (e.g. fibril microstructure and mechanical behavior) of collagen matrices or what impact these properties have on cell behavior. The present study determined the effects of varying high molecular weight HA concentration on 1) the assembly kinetics, fibril microstructure, and viscoelastic properties of 3D type I collagen matrices and 2) the response of human dermal fibroblasts, in terms of morphology, F-actin organization, contraction, and proliferation within the matrices. Results showed increasing HA concentration up to 1 mg/ml (HA:collagen ratio of 1:2) did not significantly alter fibril microstructure, but did significantly alter viscoelastic properties, specifically decreasing shear storage modulus and increasing compressive resistance. Interestingly, varied HA concentration did not significantly affect any of the measured fibroblast behaviors. These results show that HA-induced effects on collagen matrix viscoelastic properties result primarily from modulation of the interstitial fluid with no significant change to the fibril microstructure. Furthermore, the resulting biophysical changes to the matrix are not sufficient to modulate the cell-ECM mechanical force balance or proliferation of resident fibroblasts. These results provide new insight into the mechanisms by which cells sense and respond to microenvironmental cues and the use of HA in collagen-based biomaterials for tissue engineering.

Keywords

viscoelasticity; biophysical; collagen; extracellular matrix (ECM); hyaluronan; hyaluronic acid

1. Introduction

Incorporation of high molecular weight (HMW, 10^5 - 10^7 Da) hyaluronan (HA) into biomaterials is suggested to improve tissue regeneration in connective tissue and wound

healing applications (Gobbi et al., 2006; Liu et al., 1999; Park et al., 2005; Yamane et al., 2005). The goal is to mimic the high concentration of HA in connective tissue extracellular matrices (ECMs) (Fraser et al., 1997; Laurent and Fraser, 1992) or in loose, provisional matrices observed during wound healing (Chen and Abatangelo, 1999) and embryonic development (Spicer and Tien, 2004). The ECM component of these tissues represents a composite material consisting of a fibrillar network (collagen and other proteins) surrounded by an interstitial fluid containing various glycosaminoglycans (GAGs, including HA), proteoglycans (PGs), and other soluble components (growth factors, cytokines, enzymes, and diffusible molecules). In these microenvironments, HA is thought to provide cues which direct cell responses that could improve the quality of tissue regeneration. For example, persistence of HMW HA during fetal wound healing has been shown to correspond with reduced scar tissue formation, suggesting that the addition of HA might also lead to decreased scaring in adult wounds (Iocono et al., 1998; Longaker et al., 1991). However, the mechanisms by which HA influences cell behaviors and processes associated with tissue regeneration remain unclear and better understanding will improve the use of HA in biomaterial design.

One of the difficulties in elucidating how HA influences cells is that HA has been shown to influence cells through both biochemical (receptor-mediated) and biophysical (structural and mechanical) mechanisms. Biochemically, a number of different cell surface HA receptors and intracellular HA-binding proteins have been identified and linked to intracellular signaling affecting cell adhesion, migration, and proliferation (for reviews refer to Day and Prestwich, 2002; Knudson and Knudson, 1993; Turley et al., 2002). For example, HMW HA has been found to act through CD44 receptors to stimulate Akt and ERK1/2 pathways and influence human dermal fibroblast proliferation and protein synthesis, which are critical to the role of fibroblast behavior in wound healing (Croce et al., 2001; David-Raoudi et al., 2008).

In contrast to biochemical mechanisms, HA-induced biophysical signaling mechanisms remain less understood. Biophysical mechanisms translate variations in ECM microstructure and mechanics (physical properties) into localized cues that direct cell behavior through regulation of cell shape, adhesion, and cytoskeletal tension (Ghosh and Ingber, 2007). ECM microstructural organization and mechanics are determined by macromolecular composition and interactions between the insoluble collagen fibril network and the interstitial fluid phase. Mechanically, tensile loads are primarily supported by the fribrillar component and PGs/GAGs within the interstitial fluid phase contribute to the osmotic and compressive properties. For example, the negative charges on GAG chains determine the fixed charge density of the matrix which serves to increase osmotic pressure and resistance to compressive forces (Korhonen et al., 2008; Likhitpanichkul et al., 2005). HA has been shown to alter ECM physical properties, including hydration (Gerdin and Hallgren, 1997), diffusion (Coleman et al., 1998), viscoelasticity (Falcone et al., 2006; Xin et al., 2004), and collagen fibril organization (Scott, 1992). These effects have been attributed to HA's unique structure, which is often described as a long, negatively charged, non-sulfated, repeating disaccharide (glucuronic acid and N-acetyl-glucosamine) chain that coils randomly, encompassing a huge hydrodynamic domain, and fills inter-fibrillar space within the ECM (Cowman and Matsuoka, 2005; Scott et al., 1991).

Interestingly, few studies have directly linked HA-induced physical effects to cell responses. In one detailed study, an increase in glioblastoma cell migration was reported within fibrin matrices co-polymerized with HMW HA and attributed to an increase in matrix pore size (Hayen et al., 1999). Similarly, varying HA concentration within collagen matrices increased choroid fibroblast (Docherty et al., 1989) but not neutrophil (Brown, 1982) infiltration by altering the aggregation or packing of collagen fibrils. Collectively, these findings indicate that HA incorporation within biomaterials produces relevant changes in the ECM physical

properties which may serve as biophysical cues contributing to cell response and tissue regeneration.

The effect of HA incorporation within 3D collagen matrices on resident fibroblast behavior, including proliferation, morphology, migration, and matrix contraction, is a commonly used in vitro model for biomaterial design. However, the effects on fibroblast behavior have varied and it remains unclear how HA is influencing them. Increasing HA concentration within 3D collagen matrices has been reported to either increase, decrease, or not affect fibroblast proliferation, morphology, and contraction (Table 1). The majority of these studies attribute fibroblast responses to HA receptor-mediated signaling pathways. For example, Travis et al. (2001) demonstrated that HA-induced contraction of the collagen matrices by adventitial fibroblasts was CD44 but not RHAMM (receptor for hyaluronic acid-mediated motility) dependent. Indeed, several factors are known to affect HA receptor-mediated signaling and may contribute to these inconsistencies within the literature. These include 1) the molecular weight and concentration of HA (Huang et al., 2008;Moreland, 2003), 2) cell type specificity (Lokeshwar and Selzer, 2000), and 3) altered cellular susceptibility to HA, e.g. HA binding and uptake (Hall et al., 2001). However, the effects of HA on the matrix biophysical properties were not rigorously characterized in these studies and it is plausible that differences in the biophysical cues may contribute to varying fibroblast responses and inconsistencies between studies.

In previous studies, we and others have established that changes in 3D collagen matrix stiffness and fibril organization can significantly affect fibroblast behaviors (Loftis et al., 2003; Pedersen and Swartz, 2005; Pizzo et al., 2005). Furthermore, HA addition has been reported to alter the stiffness (Xin et al., 2004) and fibril organization (Docherty et al., 1989) of polymerizable collagen matrices, suggesting that HA induces biophysical cues that similarly influence fibroblast behaviors. Therefore, in this study, we identify specific physical changes induced by varying HMW HA concentration in 3D collagen matrices and correlate them with proliferation, morphology, and matrix contraction of embedded human dermal fibroblasts. The results provide new insight into 1) collagen-HA interactions as occur during collagen fibril formation (fibrillogenesis), 2) HA-induced changes in matrix viscoelastic properties, and 3) fibroblast responsiveness to HA-induced changes in matrix biophysical properties.

2. Materials and methods

2.1. Cell culture

Low passage (≤ 15 passages) foreskin-derived neonatal human dermal fibroblasts (NHDF), growth media, and passing solutions were obtained from Cambrex Bioproducts (Walkersville, MD). NHDF were propagated in fibroblast basal medium supplemented with 1 μg/ml human recombinant fibroblast growth factor, 5 mg/ml insulin, 50 mg/ml gentamicin, 50 mg/ml amphotericin B, and 2% fetal bovine serum (FBS) and maintained in a humidified atmosphere of 5% CO_2 at 37°C. Fibroblasts representing passage numbers 5 to 15 were used for all experiments.

2.2. Preparation of 3D collagen matrices

Native type I collagen prepared from acid solubilized calf skin was purchased from Sigma-Aldrich (St. Louis, MO). In some cases, type I collagen was acid solubilized and purified from pig skin by our laboratory and used to corroborate results. Collagen was dissolved in 0.01 N hydrochloric acid (HCl) and rendered aseptic for cell culture use by exposure to chloroform overnight at 4°C. Collagen concentrations were determined using a Sirius Red (Direct Red 80) assay performed as previously described (Brightman et al., 2000; Marotta and Martino, 1985).

HMW HA sodium salt prepared from bovine vitreous humor was obtained from Sigma (H7630). The average molecular weight (MW) of the HA preparation was determined by measurement of the intrinsic viscosity of HA solutions as previously described (McDonald and Levick, 1995). In brief, apparent viscosities (shear stress/shear rate) of solutions of HA in 0.1 N HCl were measured on an AR2000 rheometer (TA Instruments, New Castle, DE) with a cone and plate geometry (40mm, 2° cone angle). Viscosities of HA solutions representing concentrations of 0.25 to 3.0 mg/ml HA concentrations were measured at shear rates of 5-1000 s^{-1} at 22°C. Intrinsic viscosity [η] (ml/g) was extrapolated at zero shear rate and zero concentration using a dual extrapolation procedure from Haug and Smidsrød (1962). The weight-average molecular weight (M) was calculated using the Mark-Houwink equation, $[η] = kM^a$, where $k = 0.0279$ and $a = 0.763$ for HA in 0.1 N HCl (Cleland and Wang, 1970).

To produce 3D matrices, collagen solutions were diluted and neutralized with 10× phosphate buffered saline (PBS, 1× PBS had 0.17 M total ionic strength) and 0.1 M sodium hydroxide (NaOH) to achieve neutral pH (7.4) and a 1 or 2 mg/ml final collagen concentration. HA was added as part of the dilution volume to achieve final HA concentrations ranging from 0 to 1 mg/ml. These levels are comparable to physiologically relevant HA concentrations as occur during wound repair and within skin as well as a saturated HA:collagen weight ratio (Fraser et al., 1997; Iocono et al., 1998). Neutralized HA-collagen solutions were kept on ice prior to the induction of polymerization by warming to 37°C. For cell response studies, NHDFs were released by mild trypsinization (0.05% v/v), collected by low speed centrifugation, and added as the last component before matrix polymerization. Matrices polymerized within 15-20 minutes after which complete media was added and the constructs were maintained in a humidified atmosphere of 5% CO_2 at 37°C. Media addition was considered time zero (t_0) and media was replaced daily thereafter. All constructs remained adherent to culture chambers to mimic isometric conditions throughout time course of experimentation with the exception of fibroblast contraction analyses.

HA distribution within the collagen matrices was validated visually using alcian blue dye to selectively label HA. Collagen matrices with varied HA concentration were fixed in 4% formaldehyde and stained overnight with 0.25% alcian blue dye (Sigma) in 3% acetic acid. Matrices were visualized using brightfield microscopy and images captured on a Leica DFC480 digital camera using Leica IM50 software (Leica Microsystems, Wetzlar, Germany). Persistence of HA within collagen matrices was determined by incubating matrices in PBS (changed daily) within a tissue culture incubator (37°C and 5% CO_2 in air) for various periods up to 48 h. Matrices were then stained alcian blue. At each timepoint, duplicate sets of matrices were treated with 1000 U/ml bovine testicular hyaluronidase (HADase, H3884, Sigma) in PBS for 2 h at 37°C to digest HA prior to staining.

2.3. Analysis of collagen polymerization

A turbidity analysis was performed as described previously (Brightman et al., 2000) to evaluate the effect of HA concentration on collagen polymerization (fibrillogenesis) kinetics. Collagen solutions containing varied HA concentrations were transferred into a Lambda 35 spectrophotometer (PerkinElmer Instruments LLC, Shelton, CT) equipped with a motorized, temperature-controlled cell holder maintained at 37°C. Turbidity measurements (Absorbance at 405 nm, A_{405}) were collected at 30 s intervals for up to 2 h. Turbidity curves were used for calculation of kinetic parameters, specifically lag time (x-intercept of line tangent to the inflection point of the sigmoidal turbidity curve), polymerization rate during growth phase (slope at inflection point), final absorbance value, and polymerization half-time (time at which absorbance equals half the final absorbance value). All HA concentrations were assayed twice.

2.4. Analysis of collagen fibril microstructure

Confocal reflection microscopy (CRM; Voytik-Harbin et al., 2001) and scanning electron microscopy (SEM) were used to collect high resolution images of the 3D matrices. Collagen solutions containing varied HA concentrations were polymerized in a 4-well Lab-Tek chambered coverglass (Nalge Nunc International, Rochester, NY) or 24-well plate for CRM and SEM imaging, respectively. Confocal imaging was performed on a Bio-Rad Radiance 2100 MP Rainbow (Bio-Rad, Hemel Hempstead, UK) multiphoton/confocal system adapted to a TE2000 inverted microscope (Nikon, Tokyo, Japan). For fibril volume fraction (fibril density) measurements, confocal image stacks were collected from 3 random locations within 2 independent matrices (here "independent matrices" denotes matrices prepared separately and "replicate matrices" denotes multiple matrices/aliquots from one matrix preparation) representing each HA concentration (n = 6 images per HA concentration). Images were read into Matlab (Mathworks, Natick, MA) and binarized by thresholding. The threshold value for each image was chosen mathematically as the center of the concave bend in the sigmoidal decay curve of fibril volume fraction versus threshold value for that image. Fibril volume fraction was calculated as the percentage of fibril containing voxels to the total image voxels. For SEM analysis matrices were fixed in 3% gluteraldehyde in 0.1 M cacodylate at pH 7.4, dehydrated with ethanol, critical point dried, sputter coated with gold/palladium, and imaged at $5,000\times$ magnification using a JOEL JSM-840 SEM (Peabody, MA). Fibril diameters were measured from SEM images representing 3 to 4 random locations within 2 independent matrices for each HA concentration (totaling 60-80 fibrils). Fibril diameters, each representing the average of 5 measurements along the major axis of an individual fibril, were measured using Imaris 5.0 (Bitplane Inc., St Paul, MN).

2.5. Analysis of matrix mechanical properties

Shear and compression testing were performed on an stress-controlled AR2000 rheometer (TA Instruments, New Castle, DE) using a stainless steel 20 mm diameter parallel plate geometry. Each sample was polymerized on the rheometer by pipetting a volume (325 µl) of neutralized collagen-HA solution onto the bottom plate, lowering the geometry to a 1 mm gap distance, and then using a peltier heater in the base plate and solvent trap to maintain a 37°C, humidified environment. Matrices were allowed to polymerize in this fashion for 2.5 h. The shear modulus was then measured at frequency of 0.1 Hz and 0.01% strain, which were chosen from predetermined linear viscoelastic response regions. Shear storage (G', elastic component representing stored, recoverable energy) and loss (G'', viscous component representing energy permanently lost during deformation) moduli were calculated from the measured values of torque and phase shift (δ). Separation of the complex shear modulus into its phase components allowed more detailed analysis of the viscoelastic effects of varied HA concentration.

The effect of HA on the compressive behavior of each matrix then was evaluated by compressing (unconfined) the collagen matrix as the final stage of the rheometry protocol. Normal force was measured in response to compressive strain generated by depressing the top plate at a rate of 10 µm/s (engineering strain rate 1% /s). Stress-strain plots were generated for each sample, where compressive strain was calculated as $1 - L/L_0$ (Cauchy or engineering strain, L = height and L_0 = initial height) and stress was calculated as normal force divided by plate area (Knapp et al., 1997). Compressive moduli were calculated in two regions of the stress-strain curves (see Fig. 6). A low strain modulus was calculated by linear regression as the slope of the curve from approximately 10 to 30% strain, which is in the linear toe region. Similarly, a second modulus, termed failure modulus, was calculated in the region prior to a consistently observed failure point (Fig. 6, circles), defined where a rapid increase in stress was followed by an abrupt decline. This failure point is believed to occur when the compressive stress becomes greater than the matrix's ability to resist the hydraulic pressure, which then causes matrix collapse or detachment from the plates and an abrupt decline in stress due to

extrusion of the matrix out around the plates. Failure stress and failure strain values were taken at this point. The failure modulus was calculated by linear regression as the slope from approximately 70 to 90% failure strain. Mechanical analyses were performed on 5 independent matrices for each HA concentration (n = 5).

To demonstrate the independent contributions of HA and the collagen fibril network to viscoelastic properties, collagen matrices (2 mg/ml) with 0 or 1 mg/ml HA concentrations were treated with HADase (or PBS as control) to remove HA and then tested in unconfined compression. To enable HADase treatment, matrices were polymerized for 2 h at 37°C on a 20 mm diameter wettable surface of hydrophobic printed slides (Tekdon, Myakka City, FL) as described previously (Paderi and Panitch, 2008). Following polymerization, matrices were overlaid with 500 μl of PBS or PBS containing 1000 U/ml HADase and incubated for 4 h at 37°C. Matrices were then rinsed twice in PBS prior to testing. Slides with matrices were clamped to the rheometer stage (23°C) and a serrated 20 mm diameter parallel plate geometry lowered to the gap distance (600 μm). Matrices were subjected to unconfined compression by depressing geometry at 10 μm/s (engineering strain rate 1.67% /s) and stress-strain plots generated. Compression analysis was performed on 3 to 4 independent matrices per treatment group (n = 3-4).

2.6. Analysis of fibroblast proliferation

AlamarBlue (BioSource International, Inc., Camarillo, CA), a metabolic indicator dye, was used to indirectly measure the relative proliferation of NHDF seeded within collagen matrices with varied HA concentrations as described previously (Pizzo et al., 2005; Voytik-Harbin et al., 1998). NHDF were seeded at 5×10^4 cells/ml and matrices polymerized within 24-well plates (0.5 ml/well). Constructs remained adherent to wells throughout the assay. As a control, NHDF (same number of cells/well as gels, 2.5×10^4 cells/well) were cultured on plastic and analyzed in parallel. To evaluate for biochemical (receptor-mediated) effects of HA, varied concentrations of HA were added in the media to cells seeded on plastic. In addition, phorbol ester (PMA, phorbol myristate acetate, Sigma) was added to the media (50 ng/ml) of both plastic and matrix groups to enhance possible biochemical effects of the HA. This is based on work by Hall et al (2001) who showed that PMA, a protein kinase C (PKC) activator, addition enhanced HA binding and uptake by mouse fibroblasts, leading to a measurable biochemical response to HA. At 24 and 48 h cell number and morphology were qualitatively assessed using brightfield microscopy and culture media was replaced with fresh media containing 10% v/v alamarBlue. Media samples were collected 24 h later from each well (3×100 μl/well) into 96-well plates. Dye reduction was monitored spectrophotometrically using a SpectraMax Gemini XS plate reader (Molecular Devices, Sunnyvale, CA) with excitation and emission wavelengths of 530 and 590 nm, respectively. Sample readings were normalized by subtracting background emission (media with dye alone) and dividing by completely reduced dye emission (autoclaved sample). The assay included at least 2 independent matrices per treatment group and was repeated multiple times.

2.7. Analysis of 3D fibroblast morphology and filamentous (F)-actin organization

Collagen matrices with varied HA concentration were seeded with NHDF at 5×10^4 cells/ml and polymerized in 4-well Lab-Tek chambered coverglass (0.5 ml/well). Early after polymerization (6 h), constructs were fixed and permeabilized with 3% paraformaldehyde, 0.1% Triton 100× in PBS. NHDF were stained with Alexa Fluor 488 phalloidin (Molecular Probes, Eugene, OR) to label F-actin. Combined confocal reflection and florescence microscopy was used to collect images of cells and the surrounding collagen fibril matrix (n = 15-20 cells total from 2 independent matrices per treatment group). Images were deconvolved using AutoDeblur (Autoquant Imaging, Inc., Watervliet, NY) and analyzed in 3D using Imaris 5.0 software. Quantitative morphometric analysis was conducted using an Imaris 3D

measurement tool to measure cell length along the cell's major axis and width of the cell body at its widest point.

2.8. Analysis of matrix contraction by fibroblasts

The effect of HA concentration on matrix contraction by NHDF was evaluated using a standard collagen matrix contraction assay (Bell et al., 1979). To robustly evaluate matrix contraction, collagen concentration and cell seeding density were independently co-varied to values used in other studies (Boraldi et al., 2003; Travis et al., 2001). Collagen matrices (1 or 2 mg/ml) with varied HA concentrations were seeded with NHDF at 5, 10, or 30×10^4 cells/ml and polymerized in 24-well plates. For some experiments, PMA was added at 50 ng/ml to the media of some groups in an attempt to enhance biochemical effects of HA. Immediately following polymerization, constructs were released from wells with a tiny spatula and allowed to float in the media. Constructs were imaged at 12 to 24 h intervals over 6 days using a Leica DF480 digital camera connected to a stereo brightfield microscope (Carl Zeiss MicroImaging, Inc., Thornwood, NY). Matrix contraction was approximated as the change in surface area (% of initial surface area). Areas were measured from images in Image Pro Plus software (Media Cybernetics, Inc., Silver Spring, MD) by manually tracing the matrix perimeter (software calculated area within trace). The contraction assay was performed with 3-5 replicate matrices (aliquots of single cell-matrix preparation) per treatment group and the assay was repeated several times for each different collagen concentration–seeding density combination.

2.9. Statistical analysis

Values are reported as means ± standard deviation (SD). Statistical analyses were performed using SAS v.9.1(SAS Institute Inc, Cary, NC). To determine differences among treatment groups the general linear model (GLM) procedure was used to test analysis of variance (ANOVA), perform multiple comparisons of least-squares means using the Tukey (or Tukey-Kramer in case of unbalanced sets) method, and, where appropriate, to test for homogeneity of variances (Brown-Forsythe's test). Differences were considered statistically significant when $p < 0.05$.

3. Results

3.1. HA MW determination

The MW of HA is critical to its physio-chemical behavior and biochemical effects on cells. The MW of the HA used in the present studies was calculated from intrinsic viscosity measurements to be approximately 500 kDa. This is similar to reported values for HA extracted from bovine vitreous humor, which has been shown to contain a distribution of molecular weights (polydisperse) from 77 to 1,700 kDa with reported average MW between 200-400 kDa (Beeson et al., 2000; Laurent, 1957; Laurent et al., 1960).

3.2. Collagen polymerization kinetics are not altered by HA

Turbidimetric polymerization assays are routinely used to provide kinetic information regarding collagen fibril formation. The progressive increase in turbidity (A_{405}) as observed during collagen polymerization has been attributed to increased scattering of light by newly formed collagen fibrils (Na et al., 1986). In the present study, HA concentration was found to have no significant effect on collagen polymerization kinetics. Comparison of the turbidity curves for collagen (2 mg/ml) polymerization in the absence and presence of HA showed that all formulations demonstrated the expected sigmoidal-shaped relationship between absorbance and time with definable "lag", "growth", and "plateau" phases (Fig. 1). Furthermore, as expected, increasing the collagen concentration alone from 2 mg/ml to 3 mg/ml (Fig. 1, open squares) dramatically affected the polymerization kinetics. Specifically, the increase in

collagen concentration of 1 mg/ml decreased the polymerization half-time by 7.8 min, decreased the lag phase duration by 6.2 min, increased the polymerization rate during growth phase by 21.0×10^{-3} AU/min, and increased the final absorbance value by 0.3 AU. In contrast, the addition of HA concentrations up to 1 mg/ml, corresponding to HA:collagen ratios of 1:2, did not significantly affect the polymerization kinetics. In all cases, polymerization half-time, duration of the lag phase, polymerization rate during growth phase, and final absorbance values measured 35.8 ± 0.8 min, 25.2 ± 0.3 min, $30.4 \pm 1.6 \times 10^{-3}$ AU/min, and 0.63 ± 0.2 AU, respectively. Changes in absorbance observed at times less than 5 min, shown in Fig. 1, were interpreted as artifacts from movement or release of trapped air bubbles created during sample mixing and cuvette loading.

Microscopic analysis of collagen matrices stained with alcian blue dye verified that HA was distributed uniformly throughout the matrices in amounts that were concentration dependent (Fig. 2A). Alcian blue straining of matrices incubated in the presence of PBS for up to 2 days showed that the HA content persisted and maintained its uniform distribution within matrices (Fig. 2B). Staining intensity decreased negligibly and could be completely removed by digestion with HADase.

3.3. HA does not affect the fibril microstructure of polymerized matrices

CRM and SEM techniques were used to visually characterize the effect of varied HA concentration on the collagen fibril microstructure of formed matrices. CRM allows 3D visualization of the collagen fibril network in its natural hydrated state. Alternatively, SEM provides higher resolution images of the component collagen fibrils, but is limited to a 2D perspective and requires that the specimens be critical point dried. The resolution obtained with SEM is 1-20 nm while that obtained with CRM is 150–200 nm. Representative SEM images and CRM projections (2D overlays of image stack) of matrices with 0 and 1 mg/ml HA concentrations are shown in Fig. 3. Qualitatively, both CRM and SEM images showed no distinct changes in the density, diameter, or network organization of collagen fibrils as a result of varied HA concentration. Quantitative measures of fibril volume fraction (fibril density) and fibril diameter as determined from CRM and SEM images, respectively, were used to validate qualitative determinations. Fibril volume fraction was not significantly affected by varied HA concentration and was found to be about 6% in 2 mg/ml collagen matrices (Fig. 4A). Similarly, the mean and distribution of collagen fibril diameters were not significantly affected by varied HA concentration (histogram plot Fig. 4B). The mean fibril diameters were found to be 80.8 ± 18.3, 72.2 ± 13.0, and 72.0 ± 11.8 nm for 2 mg/ml collagen matrices prepared with 0, 0.5, and 1 mg/ml HA concentrations, respectively. Cumulatively, results from the turbidity and microstructural analyses demonstrate that the addition of HA to collagen solutions up to 50% wt/wt had no significant effect on the collagen polymerization or microstructure of the formed matrix. It should be noted that a Brown–Forsythe's test, which has increased robustness against skewed distributions compared to Levene's test, showed that the population variances were non-homogeneous (p=0.0035). In particular, this relates to the slightly larger diameters measured in matrices with decreased HA concentration and suggests that the incorporation of HA might have a slight influence in regulating fibril morphology by decreasing variance in diameter.

3.4. HA modulates the viscoelastic behavior of polymerized matrices

Oscillatory shear analysis showed that varying HA concentration significantly altered matrix viscoelasticity. Specifically, increasing HA concentration decreased shear stiffness and shifted viscoelasticity towards more viscous or fluid-like behavior. Decomposing the shear modulus into its phase components, showed that the shear storage modulus (G′), a commonly used measure of stiffness, was significantly decreased with increased HA concentration (Fig. 5A, Table 2). The highest HA concentration decreased G′ by 40%. The shear loss modulus (G″)

was found to be much smaller in magnitude than G′, indicating that the elastic (solid) phase dominates the matrix response in shear. Importantly, G″ values remained relatively constant over the range of HA concentrations tested (p=0.465, Table 2). The ratio of G″ to G′, described by the phase shift (δ, related by (tan δ = G″/G′)), reflects the behavior of the matrix between a purely viscous (fluid, δ = 90°) and purely elastic (solid, δ = 0°) material. Therefore, a significant increase in the phase shift (Fig. 5B, Table 2) indicates that increasing HA concentration shifted the viscoelasticity towards a more viscous or fluid-like material.

Unconfined compression testing showed that HA concentration significantly affected compressive behavior, indicating that HA altered fluid movement (hydraulic resistance) within the collagen matrices. Compressive loads on collagen matrices are supported primarily by the incompressibility of the interstitial fluid (Knapp et al., 1997), thus increasing resistance to fluid movement increases resistance to compression (causes increased stress). Fig 6 shows representative unconfined compression stress-strain curves for matrices with varied HA concentrations and is labeled to identify the low strain and failure moduli as well as the failure points (circles). As expected, increased HA concentration significantly increased the compressive modulus at high strains as well as failure stress and strain (Table 2). However, HA concentration did not significantly affect the low strain compressive modulus (p=0.837, Table 2). Interestingly, under the same testing conditions, varying collagen concentration (fibril density) alone alters both low and high strain compressive moduli as well as the failure stress (data not shown), indicating that the HA affected hydraulic resistance differently than collagen concentration. Further compression testing of matrices in which HA was digested and removed using HADase showed that their increased compressive resistance decreased back to values similar to control collagen matrices (no HA addition, Fig. 7). These results emphasize that HA-induced changes in matrix viscoelastic properties are largely owing to the modulation of the physio-chemical properties of the interstitial fluid phase rather than collagen fibril microstructure.

3.5. HA concentration did not affect fibroblast proliferation

As a first step in determining how collagen matrices formed with varied HA concentration affected fundamental fibroblast behavior, NHDF were entrapped (seeded) within the matrices during polymerization and their relative proliferation quantified at 24 and 48 h. Relative proliferation was measured indirectly using the metabolic indicator dye alamarBlue. In all treatment groups (1 and 2 mg/ml collagen concentrations with HA concentrations ranging from 0 to 1 mg/ml), HA concentration did not significantly affect fibroblast proliferation within the collagen matrices at either timepoint. No notable differences in cell number or viability between matrices were observed upon qualitative inspection, corroborating the alamarBlue results. Fig. 8 shows results for 1 mg/ml collagen matrices with 0, 0.5, and 1 mg/ml HA concentrations at 24 h. As expected, NHDF grown in wells on the tissue culture (TC) plastic alone showed increased proliferation compared to those grown within the 3D matrices (Pizzo et al., 2005). NHDF on plastic did not respond to HA added to the media, suggesting that the HA alone did not have a significant biochemical effect. However, as suggested by the work of Hall et al. (2001), the addition of PMA to the media did induce as significant response by NHDF to the varied HA concentration within the media. Specifically, in the presence of PMA, increased HA concentration in the media caused a decrease in fibroblast proliferation. Contrary to plastic groups, PMA added to the media of the matrix groups did not induce a significant response in the presence of varied HA concentration. Interestingly, in both matrices and on plastic, the addition of PMA alone (no HA) resulted in significantly decreased NHDF proliferation. These results demonstrate that HA alone did not have a significant biochemical effect and did not provide the necessary biophysical or biochemical cues to modulate NHDF proliferation.

3.6. HA concentration did not affect fibroblast morphology and F-actin cytoskeleton organization

Altering mechanical properties of the collagen matrices can alter the way that fibroblasts adhere and physically remodel the surrounding collagen fibril network as they attain spread, elongated morphologies. NHDF morphology was visualized and measured at a relatively early timepoint, 6 h after seeding, in attempt to capture differences in the mechanical force balance between a cell and the surrounding matrix. Surprisingly, NHDF morphology was not affected by varied HA concentration (Fig. 9). NHDF within the different HA concentration matrices had similar biopolar, spindle-shaped morphologies. Measurement (in 3D) of cell length and cell body width supported this observation. Table 3 lists the mean cell length, width, and length:width ratio for fibroblasts grown within 0 and 1 mg/ml HA concentrations which were not significantly different (p=0.06, p=0.43, p=0.06, respectively).

In addition, images of phalloidin stained NHDF were evaluated for F-actin cytoskeleton organization. Again, the addition of HA had no obvious effects on F-actin organization, in terms of filament thickness and network structure (Fig. 9C,D). As would be expected, F-actin organization correlated with cell morphology. For example, F-actin fibers were more linear and prominent in elongated cells with 2 or 3 processes (spindle shape) than in less spread cells with more processes. Comparison of cells with similar morphologies showed they had similar F-actin organization, regardless of HA concentration.

3.7. HA concentration did not affect matrix contraction by fibroblasts

Matrix contraction assays showed that varied HA concentration did not significantly affect the rate or degree of matrix contraction by NHDF (Fig. 10). Matrix contraction results from cells adhering and exerting tractional forces on the fibril network (Tamariz and Grinnell, 2002). Shown in Fig. 10A, changing the collagen concentration (1 or 2 mg/ml) and seeding density (5 or 30×10^4 cells/ml) had no significant change on the effect of varied HA concentration on matrix contraction. In an attempt to stimulate a response to HA, PMA was added to the media but also did not induce any significant effect of varied HA concentration (Fig. 10B). PMA itself appeared to slow the rate and degree of contraction, likely due to its inhibition of fibroblast proliferation. Importantly, these results correlate with the lack of differences in morphology, F-actin organization, and proliferation and further support that varied HA concentration did not affect NHDF behavior within the collagen matrices.

4. Discussion

The present study determined if varying the concentration of HMW HA (200-500 kDa) during polymerization of type I collagen altered the fibril assembly kinetics as well as the physical characteristics and cell instructive properties of resultant 3D matrices. Our experiments show that the addition of HA at the levels evaluated had no effect on the collagen polymerization kinetics or the organization of the collagen fibril network. Interestingly, the addition of HA did affect matrix mechanics largely by affecting the physio-chemical properties of the fluid phase. As a result, G′ decreased and the compressive resistance increased with increasing concentrations of HA. However, contrary to our expectation, these changes in the molecular composition and mechanical properties of the matrix did not produce measurable differences in NHDF morphology, F-actin distribution, matrix contraction, or proliferation in vitro.

Although the molecular composition of the ECM is a well-known regulator of cellular responses, physical properties of the 3D matrix are now being recognized for their instructive capacity. Recent evidence indicates that the stiffness of the ECM serves as a key regulator of fundamental cellular behaviors (Yamada and Cukierman, 2007). For example, fibroblast proliferation, spreading and motility (Pelham and Wang, 1997), as well as lineage specific

differentiation of human mesenchymal stem cells (Engler et al., 2004) have been effectively modulated by seeding cells on the surface of collagen-coated polyacrylamide gels of varying stiffness. We have also documented that NHDF entrapped within polymerizable 3D collagen matrices were able to sense and respond to changes in collagen fibril density and matrix stiffness achieved by varying collagen concentration (Pizzo et al., 2005; Roeder et al., 2002). In these studies, increasing the collagen concentration resulted in matrices with increased fibril densities and increased stiffness. The observed increase in fibril density and matrix stiffness resulted in a redistribution of cell-matrix adhesions as well as a decrease in NHDF proliferation and local matrix contraction (Pizzo et al., 2005). It is evident that modulation of the mechanical force balance between a cell and its substrate is accompanied by changes in focal adhesion composition, cell morphology, and cytoskeletal organization (Ingber, 2006).

In the present study, HA appeared to act through a different mechanism, compared to collagen concentration, to alter collagen matrix viscoelastic properties without significantly modulating fibril morphology or density. The addition of HA up to concentrations of 1 mg/ml at a HA:collagen ratio of 1:2 did not significantly alter collagen type I polymerization. Such results are consistent with work by Kuo et al. (2008) who showed that HMW HA had no effect on the polymerization kinetics of type II collagen, another member of the fibrillar collagen family. In other studies, HA has been reported to have mixed effects on the polymerization properties of type I collagen. Specifically, Tsai et al. (2006) reported that HA caused moderate changes in the assembly of pepsin-solubilized type I collagen including decreased lag time and increased polymerization rate. In a separate study involving pepsin-solubilized type I collagen, HA was found to decrease the rate of polymerization; however, these effects were highly dependent upon HA MW (Xin et al., 2004). In the present study, acid-solubilized type I collagen was chosen since this isolation technique preserves the integrity of the telopeptides, known to be critical elements of the assembly and cross-linking process, whereas enzymatic techniques involving pepsin do not (Kuznetsova and Leikin, 1999). Our findings that HA does not affect polymerization kinetics may be explained by differences in the source and molecular composition of the collagen (e.g. presence of telopeptides), polymerization reaction conditions, collagen-HA concentrations and ratios, as well as the HA MW.

HA was found to be uniformly distributed within the matrices without significantly altering the collagen fibril network organization, as visualized by CRM and SEM. These results are consistent with the idea/mechanism that HA fills the interfibrillar space and alters matrix properties through steric and/or weak interactions with collagen fibrils rather than binding or coating fibrils like other GAGs or fibronectin (Obrink, 1973; Turley et al., 1985). A moderate but not significant decrease in the variance of the fibril diameter distribution was recorded from SEM images, which might relate to HA sterically inhibiting microfibrils from coalescencing into larger fibrils (Rooney and Kumar, 1993; Tsai et al., 2006). Similar observations were made by Tsai et al. (2006) who reported a moderate narrowing of fibril diameters (measured by TEM) with increasing HA concentration and by Docherty et al. (1989) who commented on more uniform fibril diameters (measured by SEM). In the interfibrillar space, HA as well as other PGs/GAGs have been proposed to produce swelling (hydrostatic) pressure, due to their large hydrophilic domains, that is restricted by tension in the collagen fibril network (Scott, 1992; Zhu et al., 1996). In this organization, PGs are predicted to inhibit the number or strength of collagen fibril-fibril interactions (Zhu et al., 1996) and increase compressive resistance. Our mechanical testing results suggest this is happening for HA in our collagen matrices. In compression, an increased HA content resulted in an increased compressive stiffness, especially at high strain levels, as well as increased failure stress/strain. We showed that HA was directly responsible for increased compressive resistance as the effect could be reversed by selective removal of HA with HADase. In shear, the observed decrease in G′ and increase in δ with increasing HA concentration may be explained by an inhibition of fibril-fibril

interactions (collagen fibrils and network support shear and tensile loads, Sander and Barocas, 2008).

While these results show HA is altering matrix viscoelasticity but not collagen matrix microstructure, NHDF response studies show that these matrix changes do not produce significant cell instructive cues. In fact, the lack of modulation of 3D cell morphology, actin cytoskeleton organization, and matrix contractility suggested that the mechanical force balance between NHDF and their surrounding matrix was not altered by the addition of HA. NHDF did not respond to varied HA concentration, even when the collagen concentration was decreased to 1 mg/ml so that the HA:collagen ratio was 1:1. Control studies also confirmed that HA persisted within matrices for at least 2 days with no significant loss due to diffusion or degradation. These results are consistent with a previous report of only trace amounts (~2 µg/ml) of HMW HA being eluted into the media during a collagen matrix contraction assay (Mehra et al., 2006).

It was suspected that HA might create confounding biochemical and biophysical effects. However, it is unlikely that the HA had any biochemical effect as evidenced by the lack of change in NHDF proliferation when soluble HA was added as a supplement to the media. Additional evidence is provided by the PMA control groups, where PMA was added to the media in an attempt to stimulate a biochemical response to HA. PMA, a diacylglycerol analogue which activates PKC among other pathways (Brose and Rosenmund, 2002), is thought to stimulate a cell response to HA by enhancing HA binding and uptake. While the mechanism for this enhanced HA response is not yet clearly defined, it has been proposed that it occurs through CD44 and RHAMM (CD168) receptors (Hall et al., 2001; Hall et al., 2002). Here, we show that PMA induced a biochemical response to HA when NHDF were seeded within a 2D format on plastic. However, PMA was not able to induce a response to HA when NHDF were seeded within the 3D collagen matrices. These results suggest that the mechanical constraints of the 3D environment either restrict access to HA or alter the functionality of HA receptors (e.g. affect multiple ligand interactions, clustering, or co-receptors (Turley et al., 2002)). It has previously been demonstrated that cell response to HA can differ in 2D versus 3D environments (Hayen et al., 1999; Maaser et al., 1999). In summary, results from the present study demonstrate that the NHDF response was not significantly modulated by the biochemical and/ or biophysical changes induced in the matrix by the addition of HA.

Importantly, while our results evaluating NHDF response demonstrate that changes in matrix viscoelasticity are not always translated into significant biophysical cues that influence entrapped fibroblast behavior, the observed lack of a fibroblast response raises the question why HA incorporation in collagen matrices has modulated fibroblast behavior in other studies (Table 1). Certainly the possibility exists that HA has biochemical effects in those systems with those cell types. Fibroblasts from different ages (adult vs. neonatal) and tissues (foreskin vs. fetal skin) as used in the various studies have shown differences in gene expression, migration, and wound healing behaviors (Hirt-Burri et al., 2008;Meran et al., 2008). Another possibility is that the HA used in those studies induced changes in the matrix biophysical properties significant enough to influence cell behavior. It is important to note that studies performed to date have employed a wide range of collagen and HA concentrations as well as HA obtained from different sources and representing different MW. The HA used in the present work had an average MW around 200-500 kDa and was polydisperse, which upon comparison to the literature represents the mid to low end of HMW HA. It is plausible that HA representing substantially different MW (e.g. >1,000 kDa) might induce substantially different biochemical and biophysical effects on collagen matrices. In fact, HA MW dependent differences in collagen polymerization lag times (Mathews and Decker, 1968) and matrix G′ (Xin et al., 2004) have been reported. Intriguingly, 155 kDa HA, at a 10 mg/ml concentration, was found to increase G′, where as 1,200 kDa HA increased the shear rate dependence of G′ relative to

controls (Xin et al., 2004). Several studies also have reported or at least mentioned HA MW dependent differences in fibroblast behavior (Docherty et al., 1989;Huang et al., 2008). For example, Mehra et al. (2006) reported that 1,500 kDa HA, but not 190 kDa HA, resulted in increased matrix contraction. In contrast, Boraldi et al. (2003) reported that both 750 and 2,500 kDa HA did not alter matrix contraction. Differences in their experimental designs, such as 1 mg/ml HA in a 4 mg/ml collagen matrix (Boraldi) compared to 2.5 mg/ml HA in a 1.8 mg/ml collagen matrix (Mehra), suggest that HA-induced biochemical and/or biophysical cues are dependent on other experimental model parameters.

In summary, the present study provides new perspective regarding how ECM molecules, other than collagen, modulate not only the structural-mechanical properties of polymerizable collagen-based matrices but also their cell instructive capacity. Our findings show for the first time that changes in collagen matrix stiffness resulting from the modulation of fibril microstructure (e.g. fibril density and fibril-fibril cross-links) significantly affect the mechanical force balance between a cell and its surrounding matrix, while those induced by altering the physio-chemical properties of the interstitial fluid phase alone do not. Collectively, these results contribute useful design considerations that will have significant impact on the development of instructive ECM-based biomaterials for regenerative medicine and tissue engineering applications.

Acknowledgments

References

Beeson JG, Rogerson SJ, Cooke BM, Reeder JC, Chai W, Lawson AM, Molyneux ME, Brown GV. Adhesion of Plasmodium falciparum-infected erythrocytes to hyaluronic acid in placental malaria. Nat Med 2000;6:86–90. [PubMed: 10613830]

Bell E, Ivarsson B, Merrill C. Production of a tissue-like structure by contraction of collagen lattices by human fibroblasts of different proliferative potential in vitro. Proc Natl Acad Sci U S A 1979;76:1274–1278. [PubMed: 286310]

Boraldi F, Croce MA, Quaglino D, Sammarco R, Carnevali E, Tiozzo R, Pasquali-Ronchetti I. Cell-matrix interactions of in vitro human skin fibroblasts upon addition of hyaluronan. Tissue Cell 2003;35:37–45. [PubMed: 12589728]

Brightman AO, Rajwa BP, Sturgis JE, McCallister ME, Robinson JP, Voytik-Harbin SL. Time-lapse confocal reflection microscopy of collagen fibrillogenesis and extracellular matrix assembly in vitro. Biopolymers 2000;54:222–234. [PubMed: 10861383]

Brose N, Rosenmund C. Move over protein kinase C, you've got company: alternative cellular effectors of diacylglycerol and phorbol esters. J Cell Sci 2002;115:4399–4411. [PubMed: 12414987]

Brown A. Neutrophil granulocytes: adhesion and locomotion on collagen substrata and in collagen matrices. J Cell Sci 1982;58:455–467. [PubMed: 6190827]

Chen WY, Abatangelo G. Functions of hyaluronan in wound repair. Wound Repair Regen 1999;7:79–89. [PubMed: 10231509]

Cleland RL, Wang JL. Ionic polysaccharides. 3. Dilute solution properties of hyaluronic acid fractions. Biopolymers 1970;9:799–810. [PubMed: 5424507]

Coleman PJ, Scott D, Abiona A, Ashhurst DE, Mason RM, Levick JR. Effect of depletion of interstitial hyaluronan on hydraulic conductance in rabbit knee synovium. J Physiol 1998;509:695–710. [PubMed: 9596792]

Cowman MK, Matsuoka S. Experimental approaches to hyaluronan structure. Carbohydr Res 2005;340:791–809. [PubMed: 15780246]

Croce MA, Dyne K, Boraldi F, Quaglino D Jr, Cetta G, Tiozzo R, Pasquali Ronchetti I. Hyaluronan affects protein and collagen synthesis by in vitro human skin fibroblasts. Tissue Cell 2001;33:326–331. [PubMed: 11521947]

David-Raoudi M, Tranchepain F, Deschrevel B, Vincent JC, Bogdanowicz P, Boumediene K, Pujol JP. Differential effects of hyaluronan and its fragments on fibroblasts: relation to wound healing. Wound Repair Regen 2008;16:274–287. [PubMed: 18282267]

Day AJ, Prestwich GD. Hyaluronan-binding proteins: tying up the giant. J Biol Chem 2002;277:4585–4588. [PubMed: 11717315]

Docherty R, Forrester JV, Lackie JM, Gregory DW. Glycosaminoglycans facilitate the movement of fibroblasts through three-dimensional collagen matrices. J Cell Sci 1989;92:263–270. [PubMed: 2506200]

Engler A, Bacakova L, Newman C, Hategan A, Griffin M, Discher D. Substrate compliance versus ligand density in cell on gel responses. Biophys J 2004;86:617–628. [PubMed: 14695306]

Falcone SJ, Palmeri DM, Berg RA. Rheological and cohesive properties of hyaluronic acid. J Biomed Mater Res A 2006;76:721–728. [PubMed: 16315193]

Fraser JR, Laurent TC, Laurent UB. Hyaluronan: its nature, distribution, functions and turnover. J Intern Med 1997;242:27–33. [PubMed: 9260563]

Gerdin B, Hallgren R. Dynamic role of hyaluronan (HYA) in connective tissue activation and inflammation. J Intern Med 1997;242:49–55. [PubMed: 9260566]

Ghosh K, Ingber DE. Micromechanical control of cell and tissue development: implications for tissue engineering. Adv Drug Deliv Rev 2007;59:1306–1318. [PubMed: 17920155]

Gobbi A, Kon E, Berruto M, Francisco R, Filardo G, Marcacci M. Patellofemoral full-thickness chondral defects treated with Hyalograft-C: a clinical, arthroscopic, and histologic review. Am J Sports Med 2006;34:1763–1773. [PubMed: 16832129]

Greco RM, Iocono JA, Ehrlich HP. Hyaluronic acid stimulates human fibroblast proliferation within a collagen matrix. J Cell Physiol 1998;177:465–473. [PubMed: 9808154]

Hall CL, Collis LA, Bo AJ, Lange L, McNicol A, Gerrard JM, Turley EA. Fibroblasts require protein kinase C activation to respond to hyaluronan with increased locomotion. Matrix Biol 2001;20:183–192. [PubMed: 11420150]

Hall CL, Wang FS, Turley E. Src-/- fibroblasts are defective in their ability to disassemble focal adhesions in response to phorbol ester/hyaluronan treatment. Cell Commun Adhes 2002;9:273–283. [PubMed: 12745438]

Haug A, Smidsrod O. Determination of intrinsic viscosity of alginates. Acta Chem Scand 1962;16:1569–1578.

Hayen W, Goebeler M, Kumar S, Riessen R, Nehls V. Hyaluronan stimulates tumor cell migration by modulating the fibrin fiber architecture. J Cell Sci 1999;112(Pt 13):2241–2251. [PubMed: 10362554]

Hirt-Burri N, Scaletta C, Gerber S, Pioletti DP, Applegate LA. Wound-healing gene family expression differences between fetal and foreskin cells used for bioengineered skin substitutes. Artif Organs 2008;32:509–518. [PubMed: 18638304]

Huang L, Gu H, Burd A. A reappraisal of the biological effects of hyaluronan on human dermal fibroblast. J Biomed Mater Res A. 2008

Ingber DE. Cellular mechanotransduction: putting all the pieces together again. FASEB J 2006;20:811–827. [PubMed: 16675838]

Iocono JA, Krummel TM, Keefer KA, Allison GM, Paul H. Repeated additions of hyaluronan alters granulation tissue deposition in sponge implants in mice. Wound Repair Regen 1998;6:442–448. [PubMed: 9844164]

Knapp DM, Barocas VH, Moon AG, Yoo K, Petzold LR, Tranquillo RT. Rheology of reconstituted type I collagen gel in confined compression. J Rheol 1997;41:971–993.

Knudson CB, Knudson W. Hyaluronan-binding proteins in development, tissue homeostasis, and disease. FASEB J 1993;7:1233–1241. [PubMed: 7691670]

Korhonen RK, Julkunen P, Wilson W, Herzog W. Importance of collagen orientation and depth-dependent fixed charge densities of cartilage on mechanical behavior of chondrocytes. J Biomech Eng 2008;130:021003. [PubMed: 18412490]

Kuo SM, Wang YJ, Niu GC, Lu HE, Chang SJ. Influences of hyaluronan on type II collagen fibrillogenesis in vitro. J Mater Sci Mater Med 2008;19:1235–1241. [PubMed: 17701300]

Kuznetsova N, Leikin S. Does the triple helical domain of type I collagen encode molecular recognition and fiber assembly while telopeptides serve as catalytic domains? Effect of proteolytic cleavage on fibrillogenesis and on collagen-collagen interaction in fibers. J Biol Chem 1999;274:36083–36088. [PubMed: 10593890]

Laurent TC. A comparative study of physico-chemical properties of hyaluronic acid prepared according to different methods and from different tissues. Ark Kemi 1957;11:487–496.

Laurent TC, Ryan M, Pietruszkiewicz A. Fractionation of hyaluronic acid. The polydispersity of hyaluronic acid from the bovine vitreous body. Biochim Biophys Acta 1960;42:476–485. [PubMed: 13759521]

Laurent TC, Fraser JR. Hyaluronan. FASEB J 1992;6:2397–2404. [PubMed: 1563592]

Likhitpanichkul M, Guo XE, Mow VC. The effect of matrix tension-compression nonlinearity and fixed negative charges on chondrocyte responses in cartilage. Mol Cell Biomech 2005;2:191–204. [PubMed: 16705865]

Liu LS, Thompson AY, Heidaran MA, Poser JW, Spiro RC. An osteoconductive collagen/hyaluronate matrix for bone regeneration. Biomaterials 1999;20:1097–1108. [PubMed: 10382825]

Loftis MJ, Sexton D, Carver W. Effects of collagen density on cardiac fibroblast behavior and gene expression. J Cell Physiol 2003;196:504–511. [PubMed: 12891707]

Lokeshwar VB, Selzer MG. Differences in hyaluronic acid-mediated functions and signaling in arterial, microvessel, and vein-derived human endothelial cells. J Biol Chem 2000;275:27641–27649. [PubMed: 10882722]

Longaker MT, Chiu ES, Adzick NS, Stern M, Harrison MR, Stern R. Studies in fetal wound healing. V. A prolonged presence of hyaluronic acid characterizes fetal wound fluid. Ann Surg 1991;213:292–296. [PubMed: 2009010]

Maaser K, Wolf K, Klein CE, Niggemann B, Zanker KS, Brocker EB, Friedl P. Functional hierarchy of simultaneously expressed adhesion receptors: integrin alpha2beta1 but not CD44 mediates MV3 melanoma cell migration and matrix reorganization within three-dimensional hyaluronan-containing collagen matrices. Mol Biol Cell 1999;10:3067–3079. [PubMed: 10512851]

Marotta M, Martino G. Sensitive spectrophotometric method for the quantitative estimation of collagen. Anal Biochem 1985;150:86–90. [PubMed: 4083486]

Mathews MB, Decker L. The effect of acid mucopolysaccharides and acid mucopolysaccharide-proteins on fibril formation from collagen solutions. Biochem J 1968;109:517–526. [PubMed: 4234698]

McDonald JN, Levick JR. Effect of intra-articular hyaluronan on pressure-flow relation across synovium in anaesthetized rabbits. J Physiol 1995;485:179–193. [PubMed: 7658372]

Mehra TD, Ghosh K, Shu XZ, Prestwich GD, Clark RA. Molecular stenting with a crosslinked hyaluronan derivative inhibits collagen gel contraction. J Invest Dermatol 2006;126:2202–2209. [PubMed: 16741511]

Meran S, Thomas DW, Stephens P, Enoch S, Martin J, Steadman R, Phillips AO. Hyaluronan facilitates transforming growth factor-{beta}1-mediated Fibroblast Proliferation. J Biol Chem 2008;283:6530–6545. [PubMed: 18174158]

Moreland LW. Intra-articular hyaluronan (hyaluronic acid) and hylans for the treatment of osteoarthritis: mechanisms of action. Arthritis Res Ther 2003;5:54–67. [PubMed: 12718745]

Na GC, Butz LJ, Carroll RJ. Mechanism of in vitro collagen fibril assembly. Kinetic and morphological studies. J Biol Chem 1986;261:12290–12299. [PubMed: 3745187]

Obrink B. A study of the interactions between monomeric tropocollagen and glycosaminoglycans. Eur J Biochem 1973;33:387–400. [PubMed: 4266508]

Paderi JE, Panitch A. Design of a synthetic collagen-binding peptidoglycan that modulates collagen fibrillogenesis. Biomacromolecules 2008;9:2562–2566. [PubMed: 18680341]

Park SH, Park SR, Chung SI, Pai KS, Min BH. Tissue-engineered cartilage using fibrin/hyaluronan composite gel and its in vivo implantation. Artif Organs 2005;29:838–845. [PubMed: 16185347]

Pedersen JA, Swartz MA. Mechanobiology in the third dimension. Ann Biomed Eng 2005;33:1469–1490. [PubMed: 16341917]

Pelham RJ Jr, Wang Y. Cell locomotion and focal adhesions are regulated by substrate flexibility. Proc Natl Acad Sci U S A 1997;94:13661–13665. [PubMed: 9391082]

Pizzo AM, Kokini K, Vaughn LC, Waisner BZ, Voytik-Harbin SL. Extracellular matrix (ECM) microstructural composition regulates local cell-ECM biomechanics and fundamental fibroblast behavior: a multidimensional perspective. J Appl Physiol 2005;98:1909–1921. [PubMed: 15618318]

Roeder BA, Kokini K, Sturgis JE, Robinson JP, Voytik-Harbin SL. Tensile mechanical properties of three-dimensional type I collagen extracellular matrices with varied microstructure. J Biomech Eng 2002;124:214–222. [PubMed: 12002131]

Rooney P, Kumar S. Inverse relationship between hyaluronan and collagens in development and angiogenesis. Differentiation 1993;54:1–9. [PubMed: 7691668]

Sander, EA.; Barocas, VH. Biomimetic collagen tissues: collagenous tissue engineering and other applications. In: Fratzl, P., editor. Collagen: Structure and Mechanics. Springer; New York: 2008. p. 475-504.

Scott JE, Cummings C, Brass A, Chen Y. Secondary and tertiary structures of hyaluronan in aqueous solution, investigated by rotary shadowing-electron microscopy and computer simulation. Hyaluronan is a very efficient network-forming polymer. Biochem J 1991;274(Pt 3):699–705. [PubMed: 2012600]

Scott JE. Supramolecular organization of extracellular matrix glycosaminoglycans, in vitro and in the tissues. FASEB J 1992;6:2639–2645. [PubMed: 1612287]

Spicer AP, Tien JY. Hyaluronan and morphogenesis. Birth Defects Res C Embryo Today 2004;72:89–108. [PubMed: 15054906]

Tamariz E, Grinnell F. Modulation of fibroblast morphology and adhesion during collagen matrix remodeling. Mol Biol Cell 2002;13:3915–3929. [PubMed: 12429835]

Travis JA, Hughes MG, Wong JM, Wagner WD, Geary RL. Hyaluronan enhances contraction of collagen by smooth muscle cells and adventitial fibroblasts: Role of CD44 and implications for constrictive remodeling. Circ Res 2001;88:77–83. [PubMed: 11139477]

Tsai SW, Liu RL, Hsu FY, Chen CC. A study of the influence of polysaccharides on collagen self-assembly: nanostructure and kinetics. Biopolymers 2006;83:381–388. [PubMed: 16826588]

Turley EA, Erickson CA, Tucker RP. The retention and ultrastructural appearances of various extracellular matrix molecules incorporated into three-dimensional hydrated collagen lattices. Dev Biol 1985;109:347–369. [PubMed: 2581830]

Turley EA, Noble PW, Bourguignon LY. Signaling properties of hyaluronan receptors. J Biol Chem 2002;277:4589–4592. [PubMed: 11717317]

Voytik-Harbin SL, Brightman AO, Waisner B, Lamar CH, Badylak SF. Application and evaluation of the alamarBlue assay for cell growth and survival of fibroblasts. In Vitro Cell Dev Biol Anim 1998;34:239–246. [PubMed: 9557942]

Voytik-Harbin SL, Rajwa B, Robinson JP. Three-dimensional imaging of extracellular matrix and extracellular matrix-cell interactions. Methods Cell Biol 2001;63:583–597. [PubMed: 11060860]

Xin X, Borzacchiello A, Netti PA, Ambrosio L, Nicolais L. Hyaluronic-acid-based semi-interpenetrating materials. J Biomater Sci Polym Ed 2004;15:1223–1236. [PubMed: 15503636]

Yamada KM, Cukierman E. Modeling tissue morphogenesis and cancer in 3D. Cell 2007;130:601–610. [PubMed: 17719539]

Yamane S, Iwasaki N, Majima T, Funakoshi T, Masuko T, Harada K, Minami A, Monde K, Nishimura S. Feasibility of chitosan-based hyaluronic acid hybrid biomaterial for a novel scaffold in cartilage tissue engineering. Biomaterials 2005;26:611–619. [PubMed: 15282139]

Zhu W, Iatridis JC, Hlibczuk V, Ratcliffe A, Mow VC. Determination of collagen-proteoglycan interactions in vitro. J Biomech 1996;29:773–783. [PubMed: 9147974]
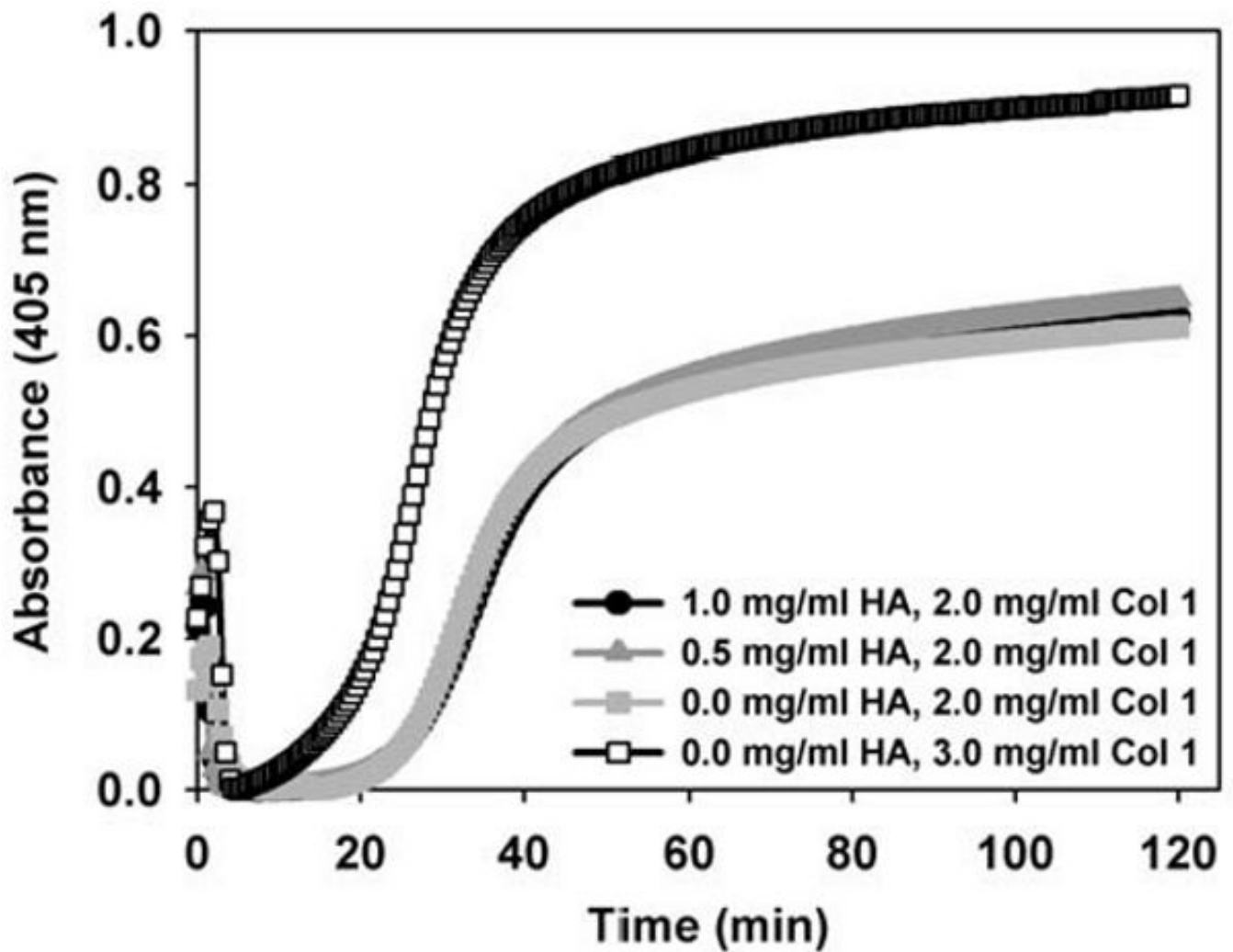
Fig. 1.
Assembly kinetics of collagen solutions (2 mg/ml) containing varied HA concentrations (0-1 mg/ml) as determined using routine turbidimetric analysis. Representative curves indicate that the addition of HA at the levels studied did not affect kinetic parameters including, duration of the half-polymerization time, duration of lag phase, polymerization rate during growth phase, or maximum absorbance. As expected, these parameters were modulated by increasing the collagen concentration from 2 mg/ml to 3 mg/ml.
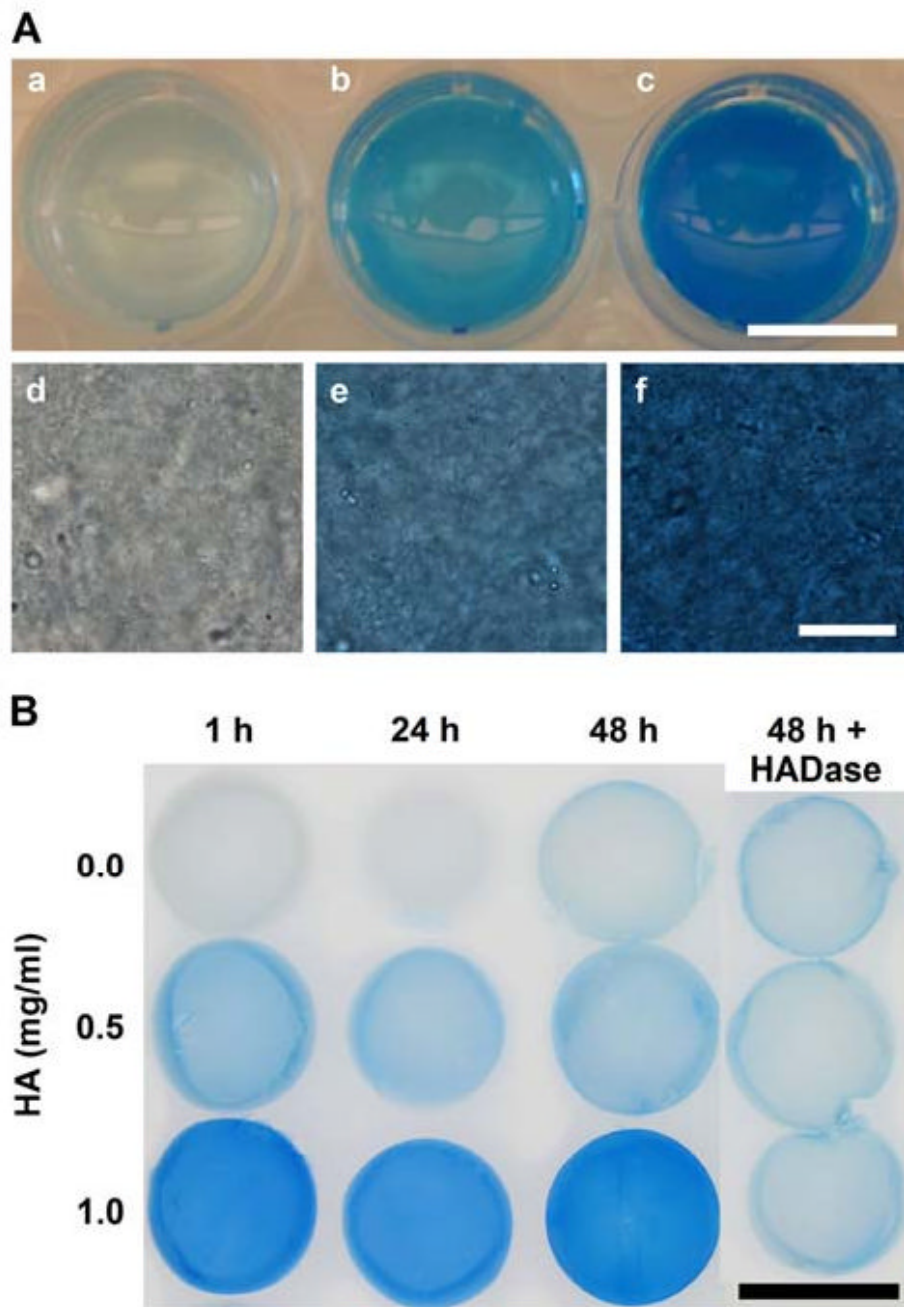
Fig. 2.
HA content and distribution within 3D collagen matrices with varied HA concentrations as visualized both macroscopically (a-c, scale bar = 1 cm) and microscopically (d-f, scale bar = 20 μm)) following staining with alcian blue dye (panel A). Alcian blue staining increased with increasing HA concentration (0 (a,d), 0.5 (b,e), and 1 (c,d) mg/ml HA in 2 mg/ml collagen matrices). HA distribution appeared homogeneous throughout the matrices. Persistence of HA within collagen matrices over time (panel B). Collagen matrices (2 mg/ml) with varied HA concentrations (0-1 mg/ml) were stained with alcian blue dye after 1, 24, and 48 h incubations at 37C with daily PBS changes (scale bar = 1 cm). Last column shows duplicate set of matrices treated with HADase to digest and remove HA prior to staining.
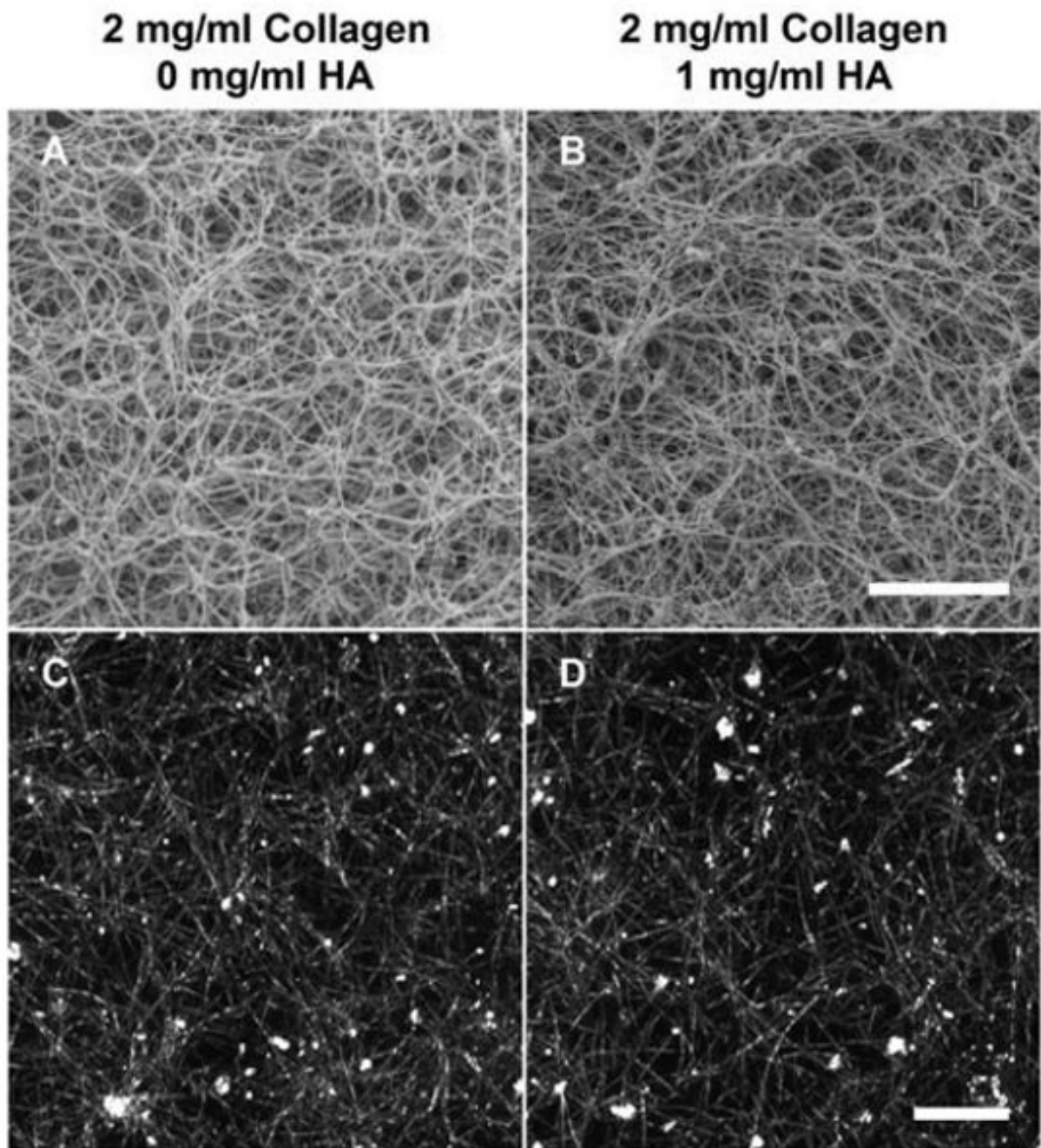
Fig. 3.
Representative SEM (A,B, scale bar = 5 μm) and CRM (C,D, scale bar = 10 μm) images showing the fibril microstructure of 3D collagen matrices (2 mg/ml) with 0 (A,C) and 1 (B,D) mg/ml HA concentrations. Qualitatively, addition of HA did not alter collagen fibril microstructure.
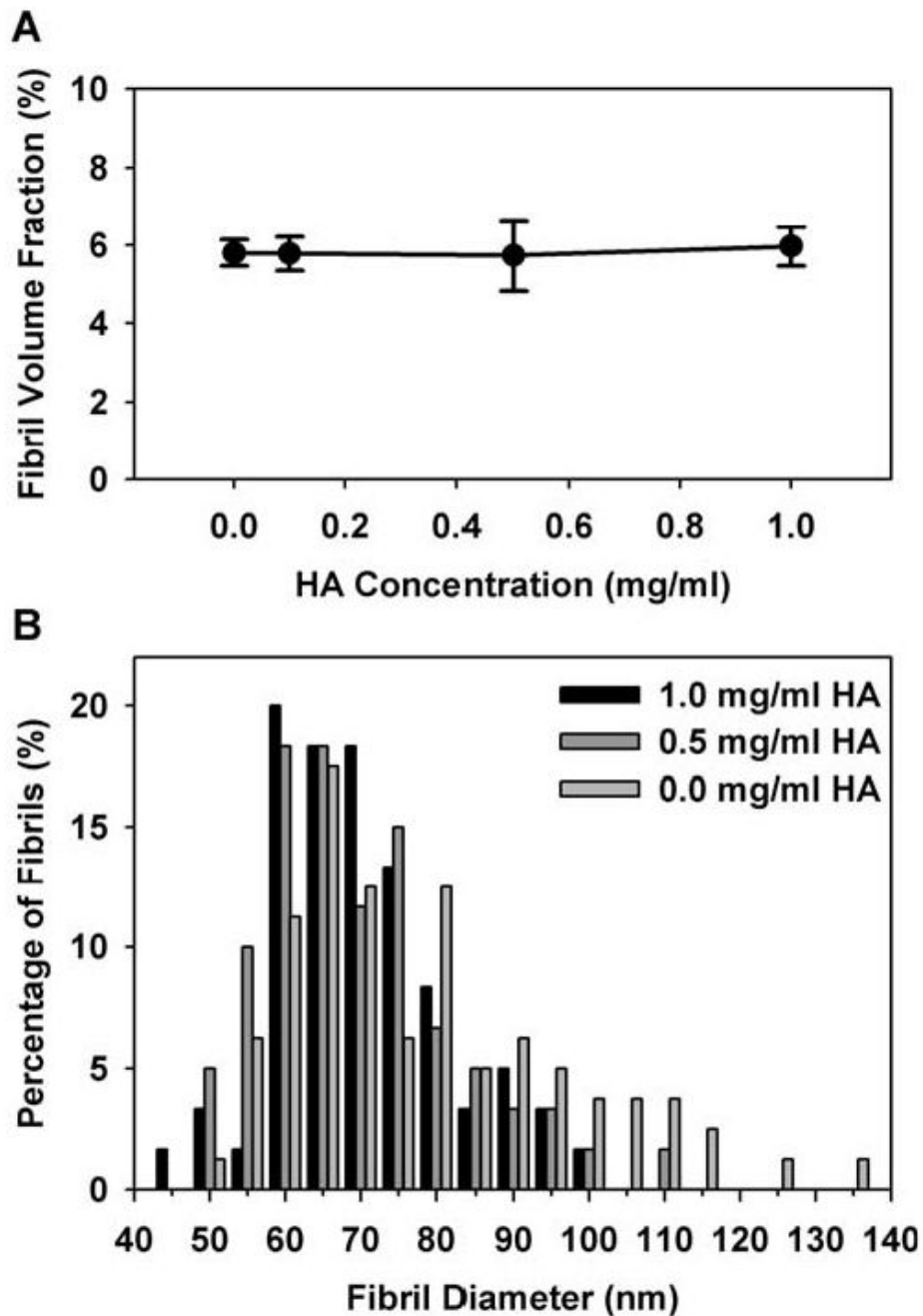
Fig. 4.
Quantitative analysis of the fibril volume fraction (A) and fibril diameter distribution (B) of collagen fibrils within 3D collagen matrices (2 mg/ml) with varied HA concentrations (0-1 mg/ml). Fibril volume fraction was measured from CRM images of 3D matrices in their natural hydrated state (n = 6 images per HA concentration). Fibril diameters (60-80 fibrils per HA concentration) were measured from high resolution SEM images. The addition of HA up to 1 mg/ml had no significant effect on fibril volume fraction or fibril diameter distribution of polymerized collagen matrices.
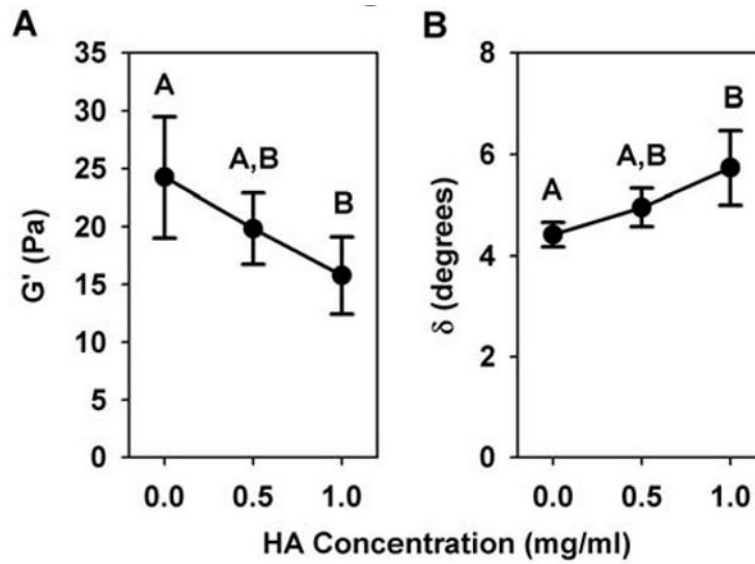
Fig. 5.
Shear storage modulus (G′, A) and phase shift (δ, B) of collagen matrices (2 mg/ml) with varied HA concentrations (0-1 mg/ml) as measured in oscillatory shear (0.01% strain, 0.1 Hz) following matrix polymerization. Increasing HA concentration significantly decreased G′ and increased δ, indicating stiffness decreased and matrices behaved more fluid-like (n = 5 independent matrices per HA concentration, different letters designate statistically different means, $p < 0.05$).
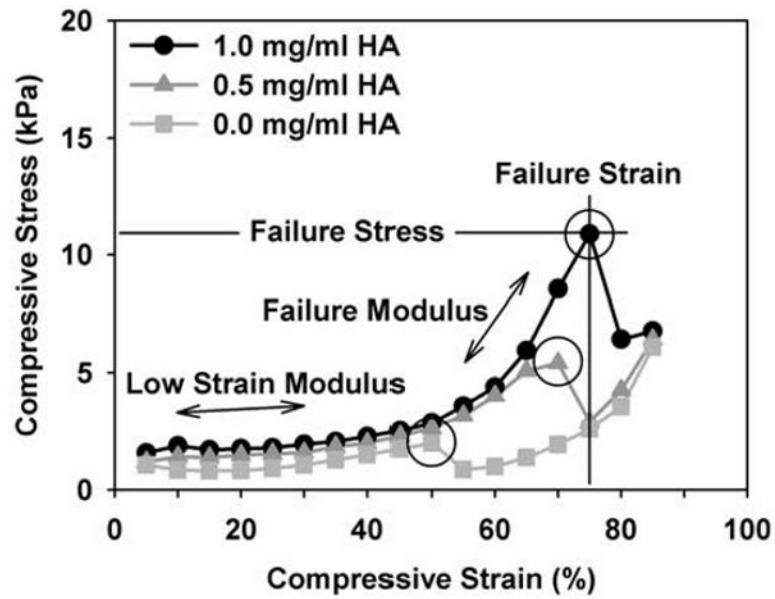
Fig. 6.
Representative unconfined compression stress-strain curves for collagen matrices (2 mg/ml) with varied HA concentrations (0-1 mg/ml). Matrices were compressed on the rheometer by depressing plate geometry at a constant rate of 10 μm/sec and measuring normal stress. Entire curves are shown to illustrate a reproducible failure point (circles) observed during testing. While an increase in failure modulus, strain, and stress were observed with increasing HA concentration, there was no significant effect on the low strain compressive modulus (parameters measured as indicated, values in Table 2).
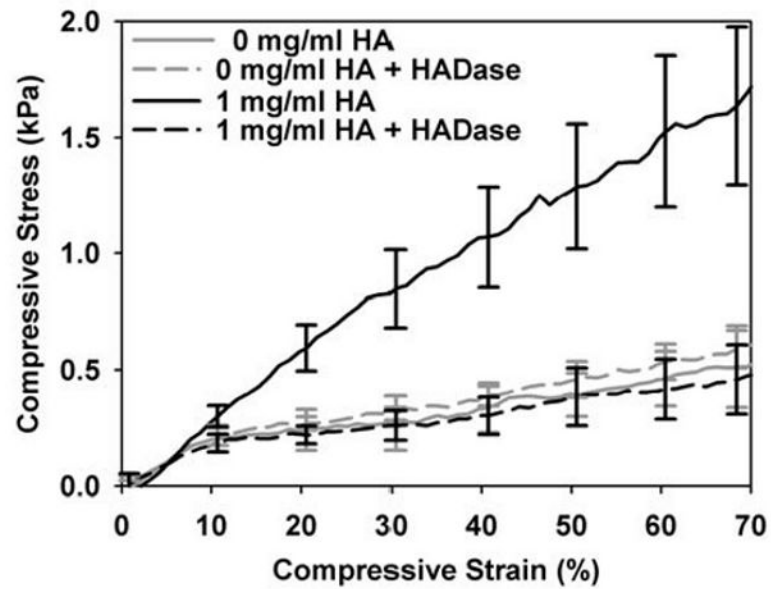
Fig. 7.
Contribution of HA to viscoelastic properties of collagen matrices. Matrices with varied HA concentrations were polymerized on slides, treated with or without HADase, and tested in unconfined compression. Compressive stress-strain curves (mean ± SD of n = 3-4 matrices per group) show that degradation of HA content within matrices decreased their increased compressive resistance back to control values (matrices with no HA).
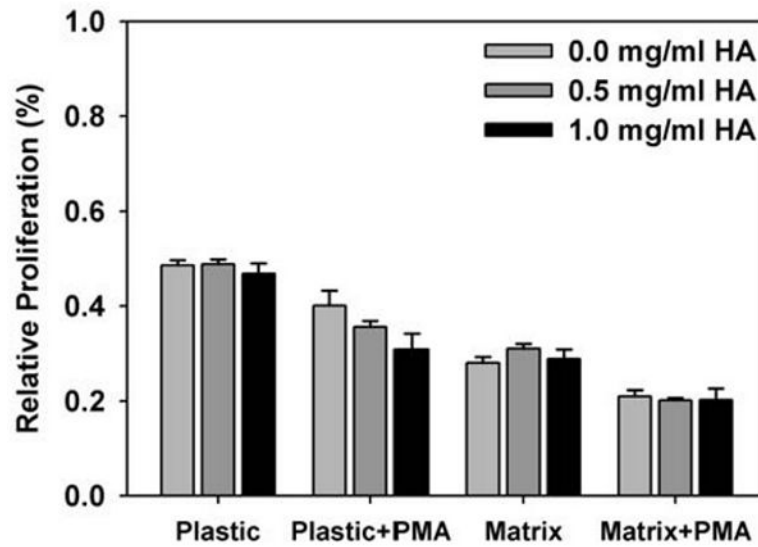
Fig. 8.
Relative proliferation, as measured by alamarBlue assay, of NHDF seeded within collagen matrices (1 mg/ml) with varied HA concentrations up to 1 mg/ml. Control analyses were simultaneously conducted for NHDF seeded on tissue culture plastic with HA added to the media and with PMA added to the media for both plastic and 3D matrix cultures (as indicated). Varied HA concentration did not significantly affect NHDF proliferation except in the case of NHDF seeded on plastic with PMA addition (bars equal mean ± SD of 2 independent matrices per treatment group from a representative assay).

0 mg/ml HA, 2 mg/ml Collagen
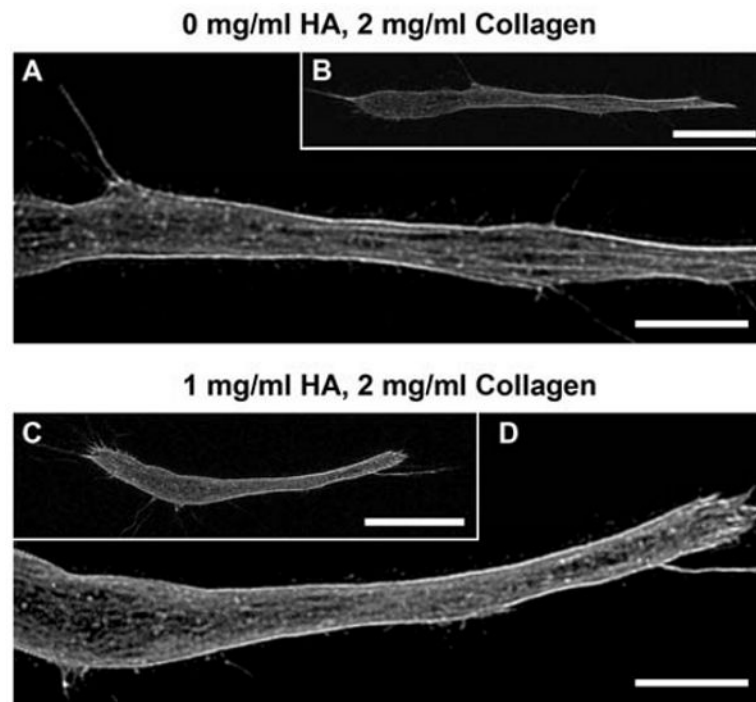

1 mg/ml HA, 2 mg/ml Collagen

Fig. 9.
Representative confocal fluorescence images of NHDF grown within collagen matrices (2 mg/ml) with 0 (A,B) and 1 (D,C) mg/ml HA concentrations and stained with Alexa Fluor 488-conjugateed phalloidin (surrounding collagen matrix not shown for clarity; B,C scale bars = 20 μm, A,D scale bars = 10 μm). Varied HA concentration did not significantly affect cell length, cell body width, or F-actin organization.
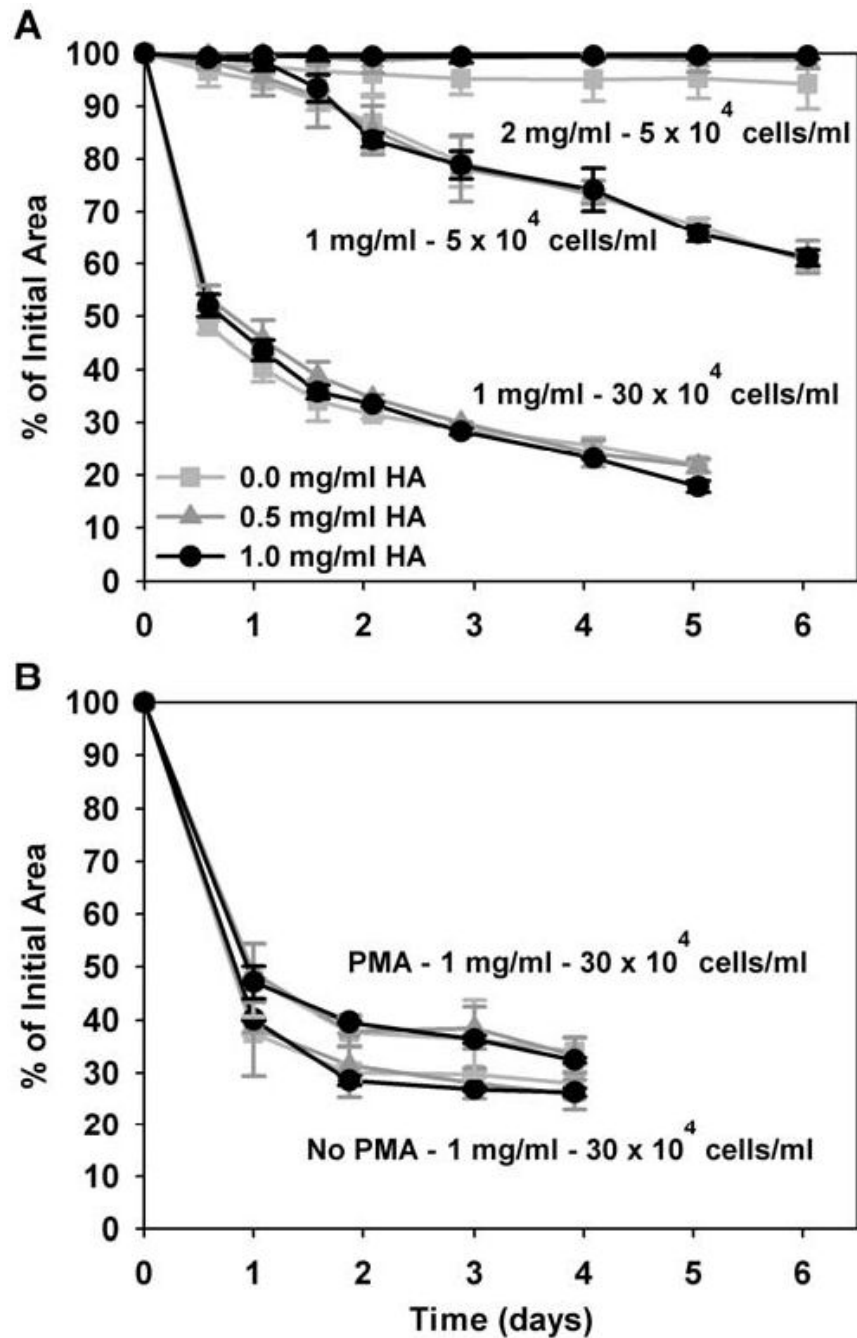
Fig. 10.
Timecourse of NHDF-mediated contraction of collagen matrices with varied HA
concentrations (0-1 mg/ml). NHDF were seeded at 5 or 30×10^4 cells/ml within 1 or 2 mg/ml
collagen matrices (as indicated in A,B) with varied HA concentrations. PMA was also added
to the media in attempt to stimulate a biochemical response to HA (B). Although NHDF
contraction varied with cell concentration, collagen concentration, and PMA addition, HA
concentration did not significantly affect the rate or degree of contraction within any of the
contexts studied (curves equal mean ± SD of 3-5 replicate matrices per treatment group from
a representative assay).

Table 1

Effects of HA concentration on fibroblast behavior within polymerizable 3D collagen matrices.

Reference	Type I Collagen Concentration (collagen source)	HA Concentration (MW)	Cell Type (seeding density)	Results: Effect of Increased HA Concentration
Greco, 1998	1.25 mg/ml (acid-solubilized rat tail prepared in lab)	0.15 mg/ml (1,100 kDa)	human dermal fibroblasts ($1.25 - 5 \times 10^4$ cells/ml)	increased cell proliferation & tubulin synthesis, but did not affect degree or rate of matrix contraction
Boraldi, 2003	4 mg/ml (acid-solubilized rat tail prepared in lab)	0 - 1 mg/ml (750 - 2,700 kDa)	human dermal fibroblasts (30×10^4 cells/ml)	did not affect matrix contraction, cell morphology, or cell distribution, but did induce thicker actin filaments
Travis, 2001	1 mg/ml (pepsin-solubilized calf skin, Vitrogen)	0 - 0.5 mg/ml (~4,000 kDa)	monkey aortic fibroblasts (30×10^4 cells/ml)	increased matrix contraction (CD44 dependent), cell spreading / elongation (not CD44 or RHAMM dependent), and pericellular collagen accumulation (CD44 dependent)
Mehra, 2006	1.8 mg/ml (Vitrogen)	0 - 2.5 mg/ml (190 & 1,500 kDa)	human dermal fibroblasts (15×10^4 cells/ml)	increased matrix contraction
Huang, 2008	1.25 mg/ml (acid-solubilized rat tail, from Gibco)	0 - 1 mg/ml (500 - 1,200 kDa)	human dermal fibroblasts (6×10^4 cells/ml)	decreased matrix contraction and cell number, affected cell morphology

Table 2

Effect of HA concentration on shear and compression mechanical properties of polymerized collagen matrices.

HA (mg/ml)	Shear Properties (mean ± SD)					Compressive Properties (mean ± SD)		
	G′ (Pa)	G″ (Pa)	δ (degrees)	Low Strain Modulus (kPa)	Failure Modulus (kPa)	Failure Stress (kPa)	Failure Strain (%)
0.0	24.3 ± 5.2	1.8 ± 0.4	4.4 ± 0.2	1.1 ± 0.4	4.8 ± 2.0	2.1 ± 0.6	48.8 ± 9.5
0.5	19.8 ± 3.1	1.7 ± 0.2	5.0 ± 0.4	1.2 ± 0.4	11.6 ± 8.3	4.7 ± 4.2	58.0 ± 11.5
1.0	15.8 ± 3.4	1.5 ± 0.4	5.7 ± 0.7	1.3 ± 0.4	41.6 ± 20.9	12.3 ± 7.0	78.8 ± 8.5

Table 3

Effect of HA concentration on fibroblast morphology within 3D collagen matrices.

HA (mg/ml)	Cell Dimensions (mean +/- SD)		
	Length (μm)	Width (μm)	Length:Width Ratio
0	123.4 ± 19.5	11.7 ± 2.9	11.1 ± 2.8
1	107.7 ± 21.9	12.6 ± 2.9	9.0 ± 2.8